



Experimental and numerical study of the distribution of a single-phase flow in a small channel heat exchanger

Frédéric Poggi, André Bontemps, Hélène Macchi-Tejeda, Alain Maréchal,
Denis Leducq

► To cite this version:

Frédéric Poggi, André Bontemps, Hélène Macchi-Tejeda, Alain Maréchal, Denis Leducq. Experimental and numerical study of the distribution of a single-phase flow in a small channel heat exchanger. IIR 1st Workshop on Refrigerant Charge Reduction, Apr 2009, Antony, France. 9 p. hal-00473268

HAL Id: hal-00473268

<https://hal.science/hal-00473268>

Submitted on 14 Apr 2010

HAL is a multi-disciplinary open access archive for the deposit and dissemination of scientific research documents, whether they are published or not. The documents may come from teaching and research institutions in France or abroad, or from public or private research centers.

L'archive ouverte pluridisciplinaire **HAL**, est destinée au dépôt et à la diffusion de documents scientifiques de niveau recherche, publiés ou non, émanant des établissements d'enseignement et de recherche français ou étrangers, des laboratoires publics ou privés.

EXPERIMENTAL AND NUMERICAL STUDY OF THE DISTRIBUTION OF A SINGLE-PHASE FLOW IN A SMALL CHANNEL HEAT EXCHANGER

F. POGGI^(a), A. BONTEMPS^(b), H. MACCHI-TEJEDA^(a), A. MARECHAL^(c), D. LEDUCQ^(a)

^(a) Cemagref, GPAN, BP 44,
Antony cedex, 92 163,, France
helene.macchi@cemagref.fr

^(b) Université Joseph Fourier, LEGI, BP 53,
Grenoble cedex 9, 38041, France
andre.bontemps@cea.fr

^(c)CEA grenoble, LITEN/DTS/LETh
Grenoble cedex 9, 38054, France
alain.marechal@cea.fr

ABSTRACT

This study focuses on the distribution of a single-phase flow in a small channel heat exchanger. A test section consisting of a cylindrical header connected to 8 multiport flat tubes of 7 parallel small channels ($D_h = 0.889$ mm) enables the measurement of singular and regular local pressure losses all along the header and the small channels, as well as the flow distribution in each small channel tube. The flat tubes are inserted up to the half of the manifold, i-e with an insertion height of 8 mm. We present and analyze the results of a header in vertical position: vertical down flow through the manifold and horizontal flow in the small channels (most of industrial applications). The experimental results are analyzed using a one-dimensional model and compared with those obtained by a numerical simulation.

RÉSUMÉ

Cette étude porte sur la distribution d'écoulements monophasiques dans un échangeur de chaleur à mini-canaux. Une section d'essais composée d'un distributeur relié à 8 barrettes de 7 mini-canaux ($D_h = 0.889$ mm) permet la mesure locale des pertes de pression singulières et régulières dans le distributeur et dans les mini-canaux, ainsi que la distribution des débits dans chaque barrette de mini-canaux. On présente et on analyse les résultats concernant la position verticale du distributeur (écoulement vertical descendant dans le distributeur et horizontal dans les mini-canaux) correspondant à la majorité des applications industrielles. Les résultats expérimentaux sont comparés à ceux obtenus par la simulation numérique ainsi qu'à ceux obtenus à l'aide d'un modèle simplifié unidimensionnel.

1. INTRODUCTION

Using compact technologies is an efficient way to enhance heat transfer in process units [1] and to reduce the refrigerant charge in refrigerating machines. For example, small-channel heat exchangers are widely used for car air-conditioning. However information about their behaviour remains scarce. Such compact heat exchangers with small channels consist of two headers or manifolds (manifold and collector) in which pressure losses are not very well known due to singularities caused by insertion of flat tubes normal to the main flow. This work aims to investigate experimentally the single-phase distribution in heat exchanger manifolds and small channels. The chosen geometry is that widely used by car manufacturers (figure 1). After its introduction in a cylindrical manifold, the refrigerant is distributed in flat aluminium multiport tubes. The distribution is mainly controlled by the pressure drop along the tubes and that related to the flow splitting in the manifold. This is the reason why the pressure drop in the manifold and the pressure drop in the small channels were carefully measured. To characterize the flow behaviour a numerical simulation has been carried out.

In addition, a one-dimensional model was realized and compared with the experimental results. Few comparable models have been proposed in the literature. These include mainly the study of Yin et al (2002)

[2] where the authors access experimentally the singularity coefficients related to the intrusion of the multiport flat tubes in the manifold through a global model. Another study is that of Maharudraya *et al* (2006) [3] where the authors investigate numerically the influence of various parameters such as the insertion of the flat tubes, the input / output position of the exchanger...

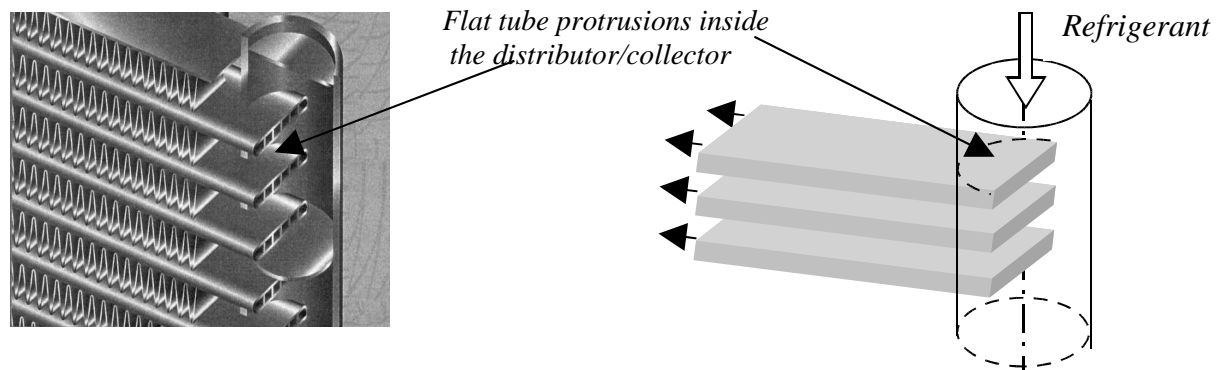


Figure1. View of an industrial small channel heat exchanger. Refrigerant path.

2. EXPERIMENTAL APPARATUS

The test section is made of transparent polycarbonate allowing us to visualize the flow distribution in the manifold and in the small channels. It consists of a 16 mm diameter and 90 mm length inlet manifold, and 8 flat tubes. Each flat tube is 230 mm long and contains 7 small channels whose hydraulic diameter is $D_h = 0.889$ mm. The flat tubes are inserted, through the wall, up to the center of the manifold. Two experiments were carried out, the first with HFE 7100 (HydroFluoroEther 7100) as working fluid, the second with water. An existing experimental test loop previously described [4] was modified to supply HFE to the inlet. A Danfoss Mass 2100 mass flowmeter ($\Delta \pm 0.033\%$) was installed at the inlet of the test section. The temperature was measured with a platinum sensor ($\Delta \pm 0.3\%$) and the pressure was measured with an absolute pressure sensor Rosemount 0/2 bars ($\Delta \pm 0.2\%$). Eight mass flowmeters allowed us to measure mass flow rates in each flat tube. The pressure loss along the manifold was measured with a Sensortechonics -5/5 mbar differential pressure sensor ($\Delta \pm P < 5$ Pa). Two other differential pressure sensors were installed: a Rosemount -10/70 mbar ($\Delta \pm 0.2\%$) for the pressure drop at the contraction between the manifold and the small channels, and a Rosemount -50/250 mbar ($\Delta \pm 0.2\%$) for the pressure drop through the small channels. The instrumentation of the test section was transferred to a high speed data logger "National instruments NI SVXI-1000" connected to a computer.

A second test loop was built to study flow distribution with water and the same instrumentation was used.

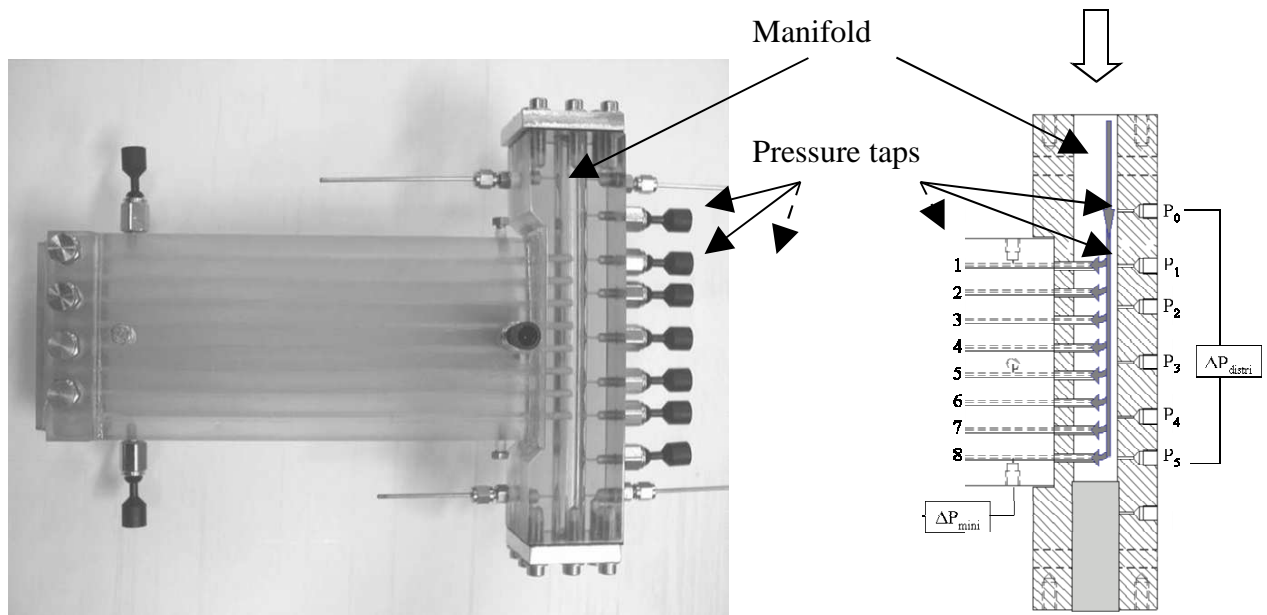


Figure 2. View of the test section

3. EXPERIMENTAL RESULTS

3.1. Distribution

The flow rate distribution within the 8 multi-port flat tubes was determined throughout the measurement of the 8 mass flowmeters at each multi-port flat tube outlet and compared to the total mass flow \dot{M}_0 . The mass flux range at the manifold inlet was varied from 15 to 500 kg/(m².s) for HFE and from 100 to 690 kg/(m².s) for water. In figure 3, the dimensionless mass flow rates \dot{m}_i / \dot{M}_0 , ($i = 1$ to 8) are presented. It is seen that the distribution is nearly homogeneous whatever the inlet mass flow rate and the fluid. It can be remarked that the maximal pressure drop in the manifold was 300 Pa and 17 000 Pa in the small channels. The ratio between the pressure drop in the channels and that in the manifold is always greater than 10. In this case the flow distribution is said to be found homogeneous [5]. The dimensionless mass flow rate is found to be about 0.125 ± 0.03 in each flat tube except for the last one where a slight increase is observed. An “accumulative pressure” forces the refrigerant towards the last multi-port flat tubes.

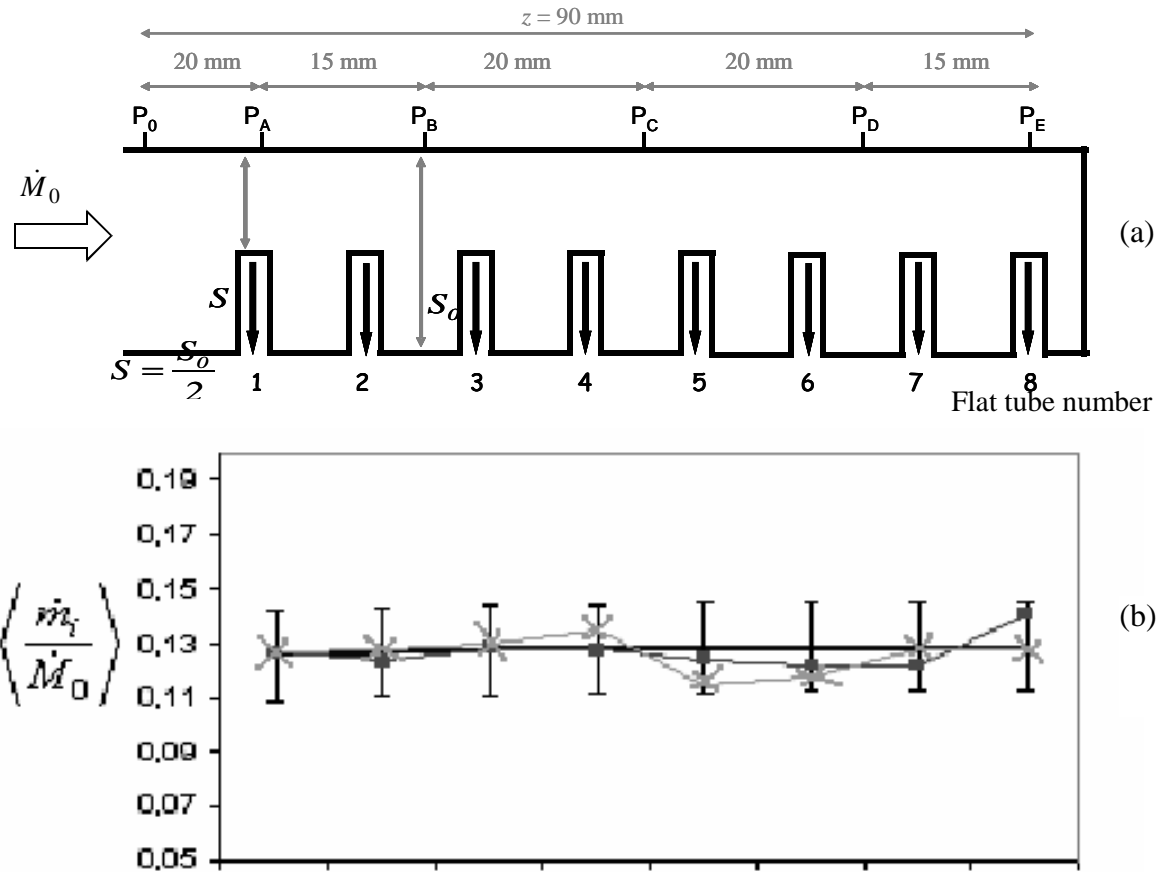


Figure 3. (a) Schematic of the manifold. (b) Experimental distribution of mass flow rates (HFE and water). The black line corresponds to numerical simulation results (Fluent).

3.2. Singular pressure losses

The flat tube protrusions inside the manifold and the presence of small channels induce many singularities with corresponding pressure drops (figures 1 and 2). In the pressure measurements, the contribution due to gravity was subtracted to obtain only the values of singular and regular pressure drops (respectively ΔP_{sing} , ΔP_{fr} , Eq. 3, 8, 11, 14 and 15). Pressure variation along the manifold is due to competition between two phenomena: a pressure increase due to progressive decrease of the mass flow rate and a pressure decrease due to regular and singular pressure losses. To distinguish one phenomenon from the other, we have studied the pressure variation (i) in feeding the eight flat tubes (figures 4, 5 a and b), (ii) in only feeding the two last flat tubes by closing the valves of the six first flat tubes (figure 4).

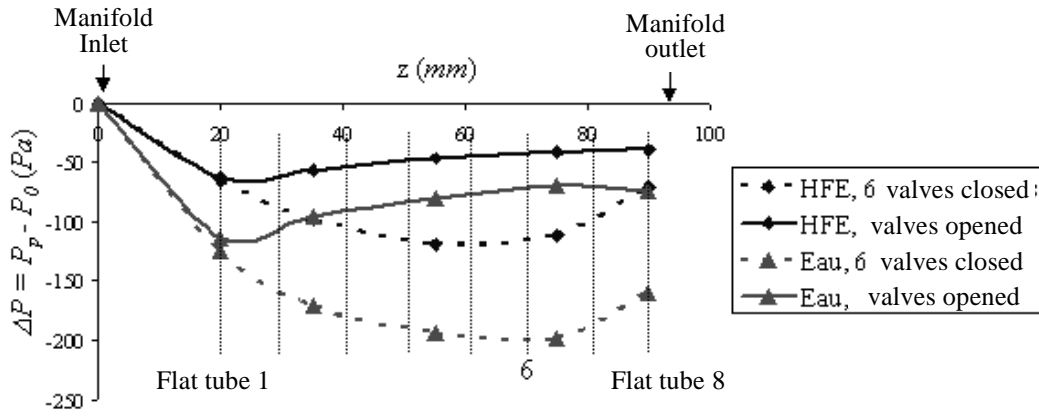


Figure 4: Pressure variation along the manifold for a 190 kg/h mass flow rate with all valves opened and with 6 closed and 2 opened valves for both fluids (HFE 7100 and water)

This second experiment allows us to determine the regular (friction) and the singular pressure losses in the first part of the manifold. By comparing both experiments (closed and opened valves) the singularity coefficient due to flow splitting can be determined (Eq. 5 to 8). After the sixth flat tube, the flow rate decrease leads to a partial compensation of these pressure losses (figure 4).

Based on experimental results with closed valves and the numerical simulation (§4), the singularity coefficients corresponding to flat tube insertions in the manifold were determined (Eq. 9 to 14).

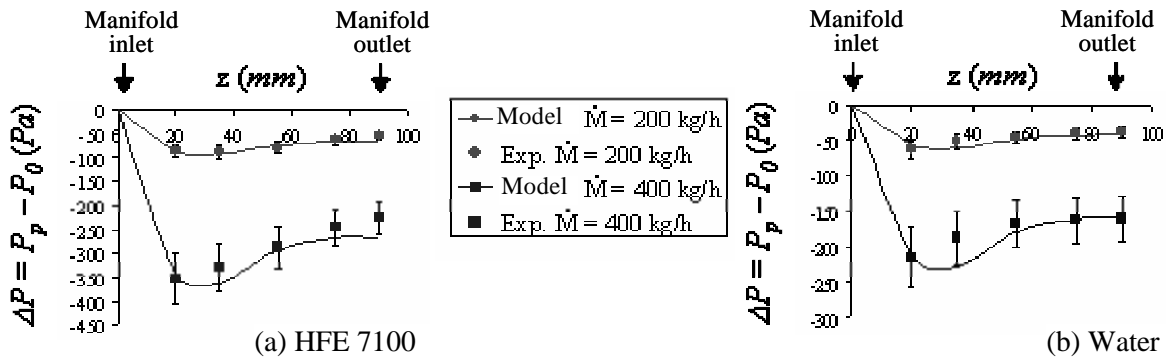


Figure 5: Pressure variation in the manifold for two mass flow rates (opened valves) with HFE 7100 (a) and water (b). Comparison between modelling and experiment

4. NUMERICAL SIMULATION

The flow behaviour and the pressure drops along the manifold have been studied by numerical simulation. Two softwares have been tested: "Comsol Multiphysics" and "Fluent". The results obtained with the two softwares are comparable and only those obtained with "Fluent" are presented. The $k-\varepsilon$ turbulence model has been chosen. The inlet velocity and a constant outlet pressure have been imposed. The numerical simulation has brought out the contraction effect caused by the insertion of the first flat tube in the manifold. Then, flow recirculation zones develop between successive flat tube intrusions, confining the main stream between the top of the flat tubes and the manifold wall (figure 6). The fluid seems to flow in a channel whose diameter would be reduced and to be submitted to small contractions and expansions. We can define a reduced cross section \bar{S} as shown in figure 7.

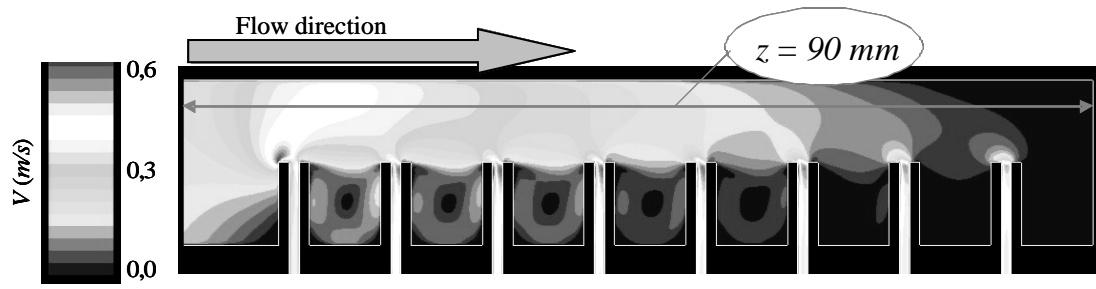


Figure 6: Numerical simulation with Fluent ($k - \varepsilon$ model) of HFE 7100 flowing in the manifold (all valves opened, mass flow rate of 223 kg/h)

5. SIMPLIFIED ONE-DIMENSIONAL MODEL

A simplified model has been developed to predict the pressure variation along the manifold. In figure 7 are represented the different zones in the manifold, as well as the calculation steps. This one-dimensional model was suggested by observations of the flow geometry obtained by numerical simulation. Singularity coefficients were then identified from experimental data introduced in this simplified model. In figures 5(a) and 5(b) are presented the model results compared to the experimental data for both fluids (HFE and water). It is observed a fair agreement between theoretical and experimental values. A slightly less good agreement with the model is obtained for the pressure drop $P_0 - P_2$, P_0 being the inlet pressure and P_2 the pressure at the flat tube number 2. Indeed, the model certainly underestimates the entrance effect due to contraction. However this difference, that increases with the mass flow rate, does not exceed 20 % with HFE and 14 % with water.

Referring to figure 3 and 7, four zones have been defined:

Zone 1 (a-b): sudden contraction at the entrance (from the whole cross-section of the manifold S_0 to $S = S_0/2$ above the top of the flat tube)

Zone 2 (b-c, e-f, ...): flow splitting between the main stream and the flow inside the flat tube

Zone 3 (c-d, f-g, ...): small enlargement between the sections S and \bar{S} above the recirculation flow

Zone 4 (d-e, g-h, ...): small contraction between \bar{S} and S

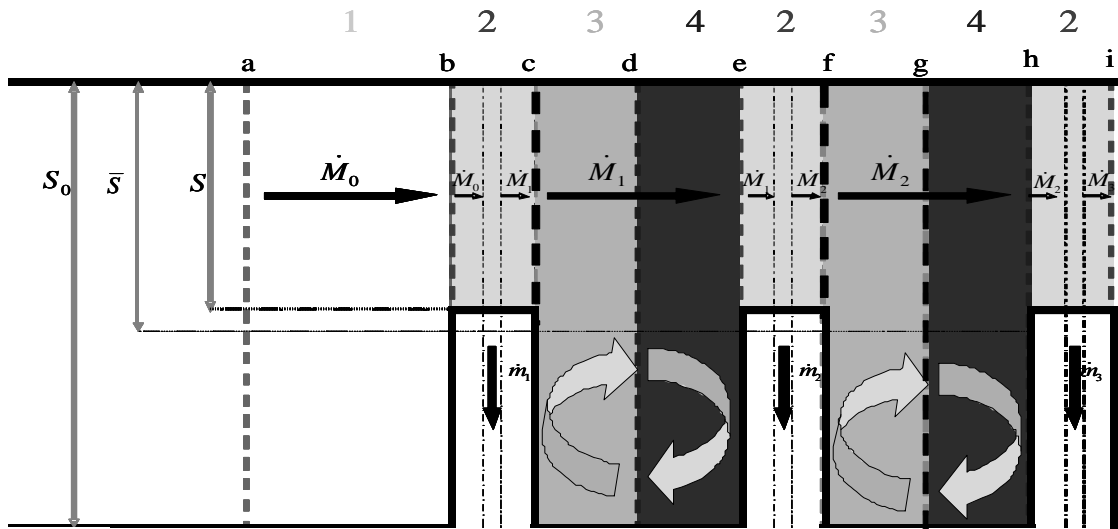


Figure 7: Definition of the different zones for one-dimensional modelling.

In each zone, the mass and momentum equations are written as following:

Zone 1.

Bernoulli equation:
$$P_a - P_b = \frac{I}{2} \rho (V_b^2 - V_a^2) + \Delta P_{fr,1} + \Delta P_{sing} \quad (1)$$

in which
$$V_a = \frac{\dot{M}_0}{\rho S_0} \quad V_b = \frac{\dot{M}_0}{\rho S} \quad \text{and} \quad S = \frac{1}{2} S_0 \quad (2)$$

$$\Delta P_{sing} = \xi_{co,1} \frac{I}{2} \rho V_b^2 \quad (3)$$

The contraction coefficient $\xi_{co,1} = f(S_0, S)$ is given by Idel'cik [6]:

$$\xi_{co,1} = 0,5(1 - S/S_0) = 0,25 \quad (4)$$

Zone 2.

Mass conservation
$$\dot{M}_0 = \dot{M}_1 + \dot{m}_1 \quad (5)$$

Bernoulli equation
$$P_b - P_c = \frac{I}{2} \rho (V_c^2 - V_b^2) + \Delta P_{fr,2} + \Delta P_T \quad (6)$$

in which
$$V_c = \frac{\dot{M}_1}{\rho S} \quad (7)$$

and the pressure loss due to flow splitting is given by

$$\Delta P_T = \xi_T \frac{I}{2} \rho V_b^2 \quad \text{with} \quad \xi_T = 0,4(1 - V_c/V_b)^2 \quad (8)$$

Zone 3.

Bernoulli equation
$$P_d - P_c = \frac{I}{2} \rho (V_c^2 - V_d^2) + \Delta P_{fr,3} + \Delta P_{sing} \quad (9)$$

with
$$V_d = \frac{\dot{M}_1}{\rho \bar{S}} \quad \text{where} \quad \frac{S}{\bar{S}} = 0,9 \quad (10)$$

$$\Delta P_{sing} = \xi_{ex} \frac{I}{2} \rho V_c^2 \quad (11)$$

The expansion coefficient $\xi_{ex} = f(S_0, S)$ is given by Idel'cik [6] and is equal to $\xi_{ex} = 0.01$.

Zone 4.

Bernoulli equation
$$P_e - P_d = \frac{I}{2} \rho (V_d^2 - V_e^2) + \Delta P_{fr,4} + \Delta P_{sing} \quad (12)$$

with
$$V_e = \frac{\dot{M}_1}{\rho S} \quad (13)$$

$$\Delta P_{sing} = \xi_{co} \frac{I}{2} \rho V_e^2 \quad (14)$$

The contraction coefficient $\xi_{co} = f(S_0, \bar{S})$ is given by Idel'cik [6] and is equal to $\xi_{ex} = 0.05$

In all equations the regular pressure losses are calculated by

$$\Delta P_{fr.,p} = 4.f \cdot \frac{G^2 \cdot z_p}{2 \cdot \rho \cdot D_h} \quad (15)$$

where z_p in the position of the p^{th} flat tube ($1 \leq p \leq 8$). The friction factor (Eq. 15) is determined from the Shah and London correlation [1] in laminar regime and the Blasius formula in turbulent regime. The regular pressure losses in the small channels have been measured [7] and it has been shown that the results obtained with conventional tubes of larger diameters are applicable for small channels as underlined in references [7, 8, 9,10]. The coefficient corresponding to the flat tube insertion inside the manifold is about 0.31 comparable to that observed in literature [11].

6. CONCLUSION

The single phase distribution in the manifold of a small channel heat exchanger was experimentally studied with two working fluids: HydroFluoroEther 7100 and water. The mass velocity was varied between 15 to 500 kg/(m².s) for HFE 7100 and 100 to 690 kg/(m².s) for water. The flow distribution was found rather homogeneous and was not depending on mass flow rate within the studied range. The fluid behaviour was determined by numerical simulation and allowed us to build a simplified one-dimensional model. The theoretical results are in fair agreement with the experimental ones.

NOMENCLATURE

D_h	hydraulic diameter, m	<i>Greek symbols</i>
f	friction factor	γ aspect ratio
G	mass velocity, $kg.(m^2.s)^{-1}$	ρ mass density, $kg.m^{-3}$
\dot{M}_0	total mass flow rate, $kg.s^{-1}$	<i>Indices and exponents</i>
\dot{m}	mass flow rate, $kg.s^{-1}$	<i>co</i> contraction
P	pressure, Pa	<i>ex</i> expansion
P_0	pressure at the manifold inlet, Pa	<i>fr</i> friction
S_0	manifold cross section, m^2	<i>i</i> flat tube number
\bar{S}	reduced manifold cross section, m^2	<i>p</i> position
z	distance along the manifold, m	<i>sing</i> singular

REFERENCES

- Shah, R. K., 2006, Advances in Science and Technology of compact heat exchangers, *Heat Transfer Engineering*, 27: 3-22.
- Yin, J.M., Bullard, C.W., Hrnjak, P.S., 2002, Single-phase pressure drop measurements in a microchannel heat exchanger, *Heat Transfer Engineering*, 23: 3-12.
- Maharudraya S., Jayanti S., Deshpande A.P., Pressure drop and flow distribution in a multiple parallel-channel configurations used in proton-exchange membrane fuel cell stacks. *Journal of Power Sources*, vol. 157, 2006, P. 358-367.
- Poggi, F., Macchi-Tejeda, H., Maréchal, A., Leducq, D., Bontemps, A., 2007, Experimental study of two-phase adiabatic flow distribution in small-channel heat exchangers. *Proceedings of International Congress of Refrigeration*, Beijing, 21 – 26 August 2007.
- Perry, R.H., Green, P.W., 1997, Chemical Engineers Handbook. Mc Graw-Hill.
- Idel'cik, I.E., 1986, Mémento des pertes de charge, EYROLLES, Paris, 494 p.
- Poggi, F., 2008, Distribution d'écoulements mono- et diphasiques et pertes de pression dans un échangeur de chaleur à mini-canaux, *Ph. D. Thesis*, Université Joseph Fourier, Grenoble.
- Morini, G.L., 2004, Single-phase convective heat transfer in microchannels: a review of experimental results. Short survey. *International Journal of Thermal Sciences* 43 (7): 631-651.
- Agostini, B. Watel, B., Bontemps, A. Thonon, B., 2004, Liquid flow friction factor and heat transfer coefficient in small channels: an experimental investigation. *Experimental Thermal and Fluid Science* 28: 97-103.

10. Bavière, R., Le Person, S., Favre-Marinet, M., Ayela, F., 2006, Les lois de l'hydrodynamique et des transferts thermiques par convection forcée aux microéchelles : Nouvelles théories ou erreurs expérimentales ? *Proceedings of Congrès SFT.2006*, 16-19 May 2006, Ile de Ré, France, 665-670.
11. Poggi, F., Macchi, H. Bontemps, A., 2007, Étude expérimentale : Distribution d'écoulements mono- et diphasique, et pertes de pression dans un échangeur à mini-canaux. *Proceedings of Congrès SFT 2007*, 29 May-1 June 2007, Île des Embiez, France, 995-1000.